

A New Pulse Shaped Frequency Division Multiplexing Technique for Doubly Dispersive Channels

Sibasish Das and Philip Schniter

Dept. EE, The Ohio State University, 2015 Neil Ave, Columbus, OH 43210
das.36@osu.edu, schniter.1@osu.edu

Abstract—There is a growing demand for higher data rate systems that can function in a highly mobile environment. This mandates designs suited to doubly selective channels. This paper presents a pulse-shaped frequency-division multiplexing (PS-FDM) scheme for transmission over doubly-dispersive channels. The pulse shapes are designed to yield an inter-symbol interference (ISI)/ inter-carrier interference (ICI) profile matching a given target response. The receiver relies on a high-performance/low-complexity equalizer based on the maximum likelihood (ML) criterion to reliably extract the transmitted symbols from the observations in the presence of controlled amounts of interference in the target response. In order to protect the transmitted information against sub-carrier nulls, a convolutional code is used at the transmitter. The equalizer exchanges soft information with a maximum *a-posteriori* probability (MAP) optimal decoder in a turbo-like fashion at the receiver. Simulations suggest that turbo-equalization with the linear complexity iterative equalizer offers significant performance enhancements over standard techniques.¹

I. INTRODUCTION

In non-trivial time- and frequency-selective environments, i.e., doubly-dispersive environments, single carrier modulation requires long and quickly-adapting equalizers for inter-symbol interference (ISI) mitigation, leading to computationally expensive receivers. Multi-carrier modulation (MCM) has thus emerged as an attractive alternative.

Orthogonal frequency-division multiplexing (OFDM) [1] is probably the most well-known MCM technique. Leveraging FFTs at the transmitter and receiver, its complexity is the lowest among spectrally-efficient MCM techniques. While the use of a cyclic prefix (CP) gives OFDM robustness to *time*-dispersive fading (at the expense of reduced spectral efficiency), CP-OFDM is often considered non-robust to *frequency*-dispersive fading, since this fading induces inter-carrier interference (ICI) in CP-OFDM (see, e.g., [2], [3] and references therein). This notion should be considered more carefully, however: while ICI mandates a more complex receiver, it also introduces beneficial Doppler-diversity [3]–[5]. In fact, [6] suggests that MCM schemes based on ICI *shaping* achieve a higher outage capacity than MCM schemes which based on ICI suppression. In other words, the benefits of ICI may outweigh the costs.

In [7], a receiver for uncoded CP-OFDM transmissions over doubly-selective channels was proposed based on max-SINR pulse shaping (for ICI control) and soft iterative ICI cancellation. The prefix and pulse lengths were constrained to prevent inter-symbol interference (ISI), leading to simplified, but suboptimal, receiver designs. In this paper, max-SINR pulse shaping is employed only at the transmitter. The receiver pulses are constrained to be rectangular. We allow arbitrary-length transmitter pulses, implying that ISI, in addition to ICI, must be controlled through pulse design and mitigated at the receiver. In addition, we relax the traditional CP length requirement (to the point of entirely removing the CP), allowing for higher spectral efficiency.

Because the bit error rate (BER) of uncoded MCM can be severely degraded by deep sub-carrier nulls, we employ coding at the transmitter and combine decoding with ICI-cancellation at the receiver. Specifically, we propose a receiver scheme that passes soft bit estimates between an equalizer and soft-input soft-output (SISO) MAP decoder in a turbo-like fashion [8]. The scheme is based on an equalizer which is related to the probabilistic data association (PDA) algorithm of [9] and similar to [10]. In contrast to [9] and [10], however, our algorithms are specifically tailored to the structure of the ISI/ICI-shaped channel.

Computer simulations were performed for a MCM system employing the SINR-maximizing pulses and the aforesaid equalization strategy. The results suggest that the performance is significantly better than standard techniques.

The paper is structured as follows. Section II describes the system model, including the pulse-shaped multi-carrier modulator, demodulator, and the doubly-dispersive channel. Section III demonstrates the SINR-optimal pulse design, while Sec. IV details the iterative receiver processing. Section V discusses the simulation results obtained, and Sec. VI concludes.

Notation: We use $(\cdot)^t$ to denote transpose, $(\cdot)^*$ conjugate, and $(\cdot)^H$ conjugate transpose. $\mathcal{C}(\mathbf{b})$ denotes the circulant matrix with first column \mathbf{b} , $\mathcal{D}(\mathbf{b})$ the diagonal matrix created from vector \mathbf{b} , and \mathbf{I}_K the $K \times K$ identity matrix. We use $[\mathbf{B}]_{m,n}$ to denote the element in the m^{th} row and n^{th} column of \mathbf{B} , where row/column indices begin with zero. \odot denotes element-wise multiplication. Expectation is denoted by $\mathbb{E}\{\cdot\}$, cross-covariance by $\Sigma_{\mathbf{b},\mathbf{c}} := \mathbb{E}\{\mathbf{b}\mathbf{c}^H\} - \mathbb{E}\{\mathbf{b}\}\mathbb{E}\{\mathbf{c}^H\}$ and

¹This work was supported by an NSF CAREER award and Motorola, Inc.

auto-covariance by $\Sigma_b := E\{\mathbf{b}\mathbf{b}^H\} - E\{\mathbf{b}\}E\{\mathbf{b}^H\}$. Finally, $\delta(\cdot)$ denotes the Kronecker delta, and \mathbb{Z} the set of integers.

II. SYSTEM MODEL

In the system considered, at each multicarrier symbol index $i \in \mathbb{Z}$, a vector of uncorrelated² bits $\mathbf{c}^{(i)} = [\mathbf{c}_0^{(i)t}, \mathbf{c}_1^{(i)t}, \dots, \mathbf{c}_{N-1}^{(i)t}]^t$, where $\mathbf{c}_k^{(i)} = [c_{k,0}^{(i)}, c_{k,1}^{(i)}, \dots, c_{k,M-1}^{(i)}]^t$ and $c_{k,m}^{(i)} \in \{0, 1\}$, is mapped to a vector of symbols, $\mathbf{s}^{(i)} = [s_0^{(i)}, s_1^{(i)}, \dots, s_{N-1}^{(i)}]^t$, $s_k^{(i)} \in \mathbb{S}$ by the symbol mapping $\psi : \{0, 1\}^M \rightarrow \mathbb{S}$, where \mathbb{S} is the constellation of size $|\mathbb{S}| = 2^M$. In this paper, \mathbb{S} is restricted to a Gray-coded PSK constellation, for simplicity. This set of N coded PSK symbols $\{s_k^{(i)}\}$ is collected to form a multicarrier symbol $\mathbf{s}^{(i)} = [s_0^{(i)}, \dots, s_{N-1}^{(i)}]^t$. These symbols are used to modulate pulsed carriers as follows:

$$t_n = \sum_{i=-\infty}^{\infty} a_{n-iN_s} \frac{1}{\sqrt{N}} \sum_{k=0}^{N-1} s_k^{(i)} e^{j\frac{2\pi}{N}(n-iN_s-N_o)k} \quad (1)$$

In (1), $\{a_n\}$ is the transmit pulse sequence, N_s is the multicarrier symbol interval, and $N_o \in \{0, \dots, N-1\}$ delays the carrier origin relative to the pulse origin. The multipath channel is described by its time-variant discrete impulse response $h_{\text{dl}}(n, l)$, defined as the time- n response to an impulse applied at time $n-l$. We assume a causal impulse response of length N_h . The signal observed by the receiver is then

$$r_n = \nu_n + \sum_{l=0}^{N_h-1} h_{\text{dl}}(n, l)t_{n-l} \quad (2)$$

where ν_n denotes samples of circular white Gaussian noise (CWGN) with variance σ^2 . Defining $r_n^{(i)} := r_{iN_s+n}$, $\nu_n^{(i)} := \nu_{iN_s+n}$, and $h_{\text{dl}}^{(i)}(n, l) := h_{\text{dl}}(iN_s+n, l)$, it can be shown that

$$\begin{aligned} r_n^{(i)} &= \nu_n^{(i)} + \sum_{l=0}^{N_h-1} h_{\text{dl}}^{(i)}(n, l) \sum_{\ell=-\infty}^{\infty} a_{\ell N_s+n-l} \\ &\times \frac{1}{\sqrt{N}} \sum_{k=0}^{N-1} s_k^{(i-\ell)} e^{j\frac{2\pi}{N}(n-l+\ell N_s-N_o)k} \end{aligned} \quad (3)$$

To estimate the multicarrier symbol $\mathbf{s}^{(i)}$, the receiver employs the pulse $\{b_n\}$ as follows:

$$x_d^{(i)} = \frac{1}{\sqrt{N}} \sum_n r_n^{(i)} b_n e^{-j\frac{2\pi}{N}d(n-N_o)} \quad (4)$$

Here again N_o delays the carrier origin relative to the pulse origin. Specifically, $\{b_n\}_{n=0}^{N_b-1}$ is defined as

$$b_n = \begin{cases} 0, & 0 \leq n < N_h - 1 \\ \sqrt{\frac{N_s}{N}}, & N_h \leq n < N + N_h \\ 0, & N + N_h \leq n \leq N_b \end{cases} \quad (5)$$

Note that this system reduces to CP-OFDM with $N_o = N_s - N$, $\{a_n\}_{n=0}^{N_s-1} = 1$ and $N_a = N_b = N_s$. Note also that $N_g := N_s - N$ is analogous to CP-OFDM guard interval.

²If coding is employed, then $\mathbf{c}^{(i)}$ is an interleaved vector of coded bits.

Plugging (3) into (4), we find

$$x_d^{(i)} = w_d^{(i)} + \sum_{\ell} \sum_{k=0}^{N-1} h_{\text{df}}^{(i,\ell)}(d-k, k) s_k^{(i-\ell)} \quad (6)$$

where

$$w_d^{(i)} := \frac{1}{\sqrt{N}} \sum_n b_n \nu_n^{(i)} e^{-j\frac{2\pi}{N}d(n-N_o)} \quad (7)$$

$$\begin{aligned} h_{\text{df}}^{(i,\ell)}(d, k) &:= \frac{1}{N} \sum_n \sum_{l=0}^{N_h-1} h_{\text{dl}}^{(i)}(n, l) b_n a_{\ell N_s+n-l} e^{-j\frac{2\pi}{N}d(n-N_o)} \\ &\times e^{-j\frac{2\pi}{N}k(l-\ell N_s)} \end{aligned} \quad (8)$$

Equation (6) indicates that $h_{\text{df}}^{(i,\ell)}(d, k)$ can be interpreted as the response, at time i and subcarrier $k+d$, to a frequency-domain impulse applied at time $i-\ell$ and subcarrier k .

In practice, we implement finite-duration causal pulses $\{a_n\}$ of length N_a implying that only a finite number of terms in the set $\{h_{\text{df}}^{(i,\ell)}(d, k), \ell \in \mathbb{Z}\}$ will be non-zero. Specifically, (8) implies that non-zero terms result from indices ℓ which satisfy $0 \leq \ell N_s + n - l \leq N_a - 1$ for some $n \in \{0, \dots, N_b - 1\}$ and some $l \in \{0, \dots, N_h - 1\}$. It is straightforward to show that $h_{\text{df}}^{(i,\ell)}(d, k)$ is non-zero for $\ell \in \{-L_{\text{pre}}, \dots, L_{\text{pst}}\}$ where $L_{\text{pre}} = -\lfloor \frac{N+N_h-1}{N_s} \rfloor$ and $L_{\text{pst}} = \lfloor \frac{N_a-2}{N_s} \rfloor$ for $\{b_n\}$ in (5).

With the definitions $\mathbf{x}^{(i)} := [x_0^{(i)}, \dots, x_{N-1}^{(i)}]^t$, $\mathbf{w}^{(i)} := [w_0^{(i)}, \dots, w_{N-1}^{(i)}]^t$, and $[\mathbf{H}^{(i,\ell)}]_{d,k} := h_{\text{df}}^{(i,\ell)}(d-k, k)$, (6) implies the linear time-varying (LTV) multiple-input multiple-output (MIMO) system

$$\mathbf{x}^{(i)} = \mathbf{w}^{(i)} + \sum_{\ell=-L_{\text{pre}}}^{L_{\text{pst}}} \mathbf{H}^{(i,\ell)} \mathbf{s}^{(i-\ell)}. \quad (9)$$

In the sequel we assume wide-sense stationary uncorrelated scattering (WSSUS) [11] so that $E\{h_{\text{dl}}(n, l)h_{\text{dl}}^*(n-q, l-m)\} = r_t(q)\sigma_l^2\delta(m)$. Here, $r_t(q)$ denotes the normalized autocorrelation (i.e., $r_t(0) = 1$) and σ_l^2 the variance of the l^{th} lag.

III. PULSE DESIGN

The choice of $\{a_n\}$ and $\{b_n\}$ affect the ISI/ICI patterns of the MIMO system (9). For example, the CP-OFDM choices yield a system for which ISI and ICI vanish if the channel is LTI with delay spread $N_h \leq N_s - N + 1$. When the channel is LTV, however, no choice of $\{a_n\}$ and $\{b_n\}$ is capable of completely suppressing both ISI and ICI. In this paper, our strategy is to choose $\{a_n\}$ (with $\{b_n\}$ fixed to the CP-OFDM receiver window (5)) so as to impart a particular structure to the effective channel response $\mathbf{H}^{(i,\ell)}$. The ideal target ICI/ISI pattern should allow high-performance/low-complexity equalization while being (nearly) attainable for some choice of $\{a_n\}$. We use the optimality criterion defined in [12] to design pulse $\{a_n\}$. We focus on an ICI/ISI target that has a ‘‘cursor’’ coefficient $\mathbf{H}^{(i,0)}$ with the banded structure illustrated in Fig. 1 and ISI coefficients $\{\mathbf{H}^{(i,\ell)}\}_{\ell \neq 0}$ which equal zero. This choice is motivated by the low-pass nature of typical Doppler spectra (see [7]) and assumes that ISI can be effectively suppressed.

(With very long delay spread, it may be more appropriate to design pulses which allow post-cursor ISI and apply block decision feedback equalization; this is discussed in [12].) The width of the band in Fig. 1 is proportional to design parameter D . When Rayleigh fading with maximum normalized Doppler frequency f_d is assumed, *i.e.*, $r_1(q) = J_0(2\pi f_d q)$, we choose $D \approx \lceil f_d N \rceil$.

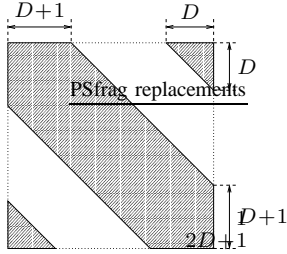


Fig. 1. Desired structure of MIMO cursor coefficient $\mathbf{H}^{(i,0)}$.

We design pulses according to the SINR($\mathbf{x}^{(i)}$) := $\mathcal{E}_s/\mathcal{E}_{ni}$ criterion, where signal energy \mathcal{E}_s and noise-plus-interference energy \mathcal{E}_{ni} are defined relative to the target. If we define $\mathcal{E}_{s,d}$ to be the energy contributed by $s_d^{(i)}$ to $x_d^{(i)}$, and if we define $\mathcal{E}_{ni,d}$ to be the energy contributed to $x_d^{(i)}$ by additive noise $w_d^{(i)}$, non-cursor symbols $\{s_d^{(j)}\}_{j \neq i}$, and non-neighboring co-cursor symbols $\{s_k^{(i)}\}_{k=0}^{d-D-1} \cup \{s_k^{(i)}\}_{k=d+D+1}^{N-1}$, then $\mathcal{E}_s = \sum_d \mathcal{E}_{s,d}$ and $\mathcal{E}_{ni} = \sum_d \mathcal{E}_{ni,d}$. Note that the energy contributed to $x_d^{(i)}$ by neighboring co-cursor symbols $\{s_k^{(i)}\}_{k=d-D}^{d-1} \cup \{s_k^{(i)}\}_{k=d+1}^{d+D}$ is considered neither signal nor interference, but rather a “don’t care” quantity. In choosing $\mathbf{a} := [a_0, \dots, a_{N_a-1}]^t$, we impose the average transmitted power constraint $\|\mathbf{a}\|^2 = N_s$, consistent with CP-OFDM. Here we present a summary of the pulse shape derivation. The details can be found in [12].

From (6), (8), the description above and our WSSUS assumption it can be shown that

$$\mathcal{E}_s = \frac{1}{N} \mathbf{a}^H (\mathbf{R}_a \odot \mathbf{B}_s) \mathbf{a}, \quad (10)$$

where \mathbf{R}_a and \mathbf{B}_s are $N_a \times N_a$ matrices, defined element-wise as $[\mathbf{R}_a]_{p,q} := r_1(q-p)$, and $[\mathbf{B}_s]_{p,q} := \sum_{l=0}^{N_h-1} \sigma_l^2 b_{q+l} b_{p+l}^*$. From (6) and our definition of $\mathcal{E}_{ni,d}$, it can be shown that

$$\mathcal{E}_{ni} = \mathbf{a}^H (\sigma^2 \mathbf{I}_{N_a} + \mathbf{R}_a \odot \mathbf{C}_a \odot \mathbf{B}_t - \mathbf{R}_a \odot \mathbf{D}_a \odot \mathbf{B}_s) \mathbf{a} \quad (11)$$

In (11), \mathbf{C}_a , \mathbf{D}_a , and \mathbf{B}_t are $N_a \times N_a$ matrices defined element-wise as $[\mathbf{D}_a]_{p,q} := \frac{1}{N} \sin(\frac{\pi}{N}(2D+1)(q-p)) / \sin(\frac{\pi}{N}(q-p))$, $[\mathbf{B}_t]_{p,q} := \sum_{\ell=-L_{pre}}^{L_{pst}} \sum_{l=0}^{N_h-1} \sigma_l^2 b_{q+l-\ell} b_{p+l-\ell}^*$, and $[\mathbf{C}_a]_{p,q} := \delta((q-p)_N)$. We use $\|\mathbf{a}\|^2 = \|\mathbf{b}\|^2 = N_s$ to write (11). The optimization SINR = $\mathcal{E}_s/\mathcal{E}_{ni}$ with respect to \mathbf{a} under the constraint $\|\mathbf{a}\|^2 = N_s$, can be written as (12), where $\mathbf{v}_*(\mathbf{M}, \mathbf{N})$ denotes the principle generalized eigenvector of the matrix pair (\mathbf{M}, \mathbf{N}) . The optimization can be carried out in advance for Rayleigh fading. The pulse $\{a_n\}$ depends on maximum Doppler frequency, power profile, and noise variance. Typical pulses generated can be seen in Fig. 2(a)-(b).

$$\begin{aligned} \mathbf{a}_* &= \arg \max_{\mathbf{a}: \|\mathbf{a}\|^2 = N_s} \frac{\mathbf{a}^H (\mathbf{R}_a \odot \mathbf{B}_s) \mathbf{a}}{\mathbf{a}^H (\sigma^2 \mathbf{I} + \mathbf{R}_a \odot \mathbf{C}_a \odot \mathbf{B}_t - \mathbf{R}_a \odot \mathbf{D}_a \odot \mathbf{B}_s) \mathbf{a}} \\ &= \frac{\mathbf{v}_*(\mathbf{R}_a \odot \mathbf{B}_s, \sigma^2 \mathbf{I} + \mathbf{R}_a \odot \mathbf{C}_a \odot \mathbf{B}_t - \mathbf{R}_a \odot \mathbf{D}_a \odot \mathbf{B}_s)}{N^{-1/2}} \quad (12) \end{aligned}$$

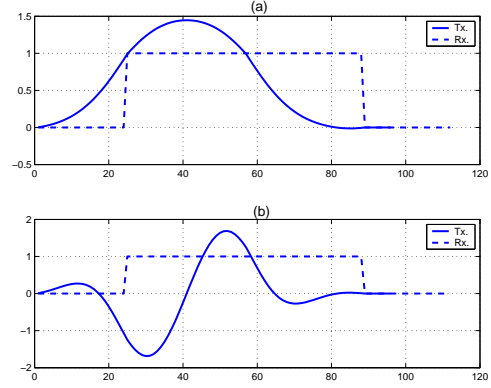


Fig. 2. Typical SINR-optimal pulse shapes generated when (a) $f_d = 0.01$, $SNR = 2\text{dB}$, and (b) $f_d = 0.03$, $SNR = 2\text{dB}$.

IV. ITERATIVE EQUALIZATION

Here we develop a low complexity algorithm that extracts information about the bits $c^{(i)}$ from the observation $\mathbf{x}^{(i)}$ while leveraging the sparse channel structure that results from SINR-optimal pulse design.

IV.1) Simplified System Model: With proper application of the pulse shapes described in Sec. III, the MIMO channel $\{\mathbf{H}^{(i,\ell)}\}_{\ell=-L_{pre}}^{L_{pst}}$ has negligible pre- and post-cursor ISI and a cursor coefficient $\mathbf{H}^{(i,0)}$ with the banded structure shown in Fig. 1. This structure implies that $s_k^{(i)}$ will contribute primarily to the observation elements $\{x_d^{(i)}\}_{d=k-D}^{k+D}$, where all indexing in this section is taken modulo- N . Thus, good “local” estimates of $s_k^{(i)}$ can be generated using $\mathbf{x}_k^{(i)} := [x_{k-D}^{(i)}, \dots, x_{k+D}^{(i)}]^t$. If we define $\mathbf{s}_k^{(i)} := [s_{k-2D}^{(i)}, \dots, s_{k+2D}^{(i)}]^t$, $\mathbf{w}_k^{(i)} := [w_{k-D}^{(i)}, \dots, w_{k+D}^{(i)}]^t$, and $\boldsymbol{\varepsilon}_k^{(i)} := [\varepsilon_{k-D}^{(i)}, \dots, \varepsilon_{k+D}^{(i)}]^t$, then we can write

$$\mathbf{x}_k^{(i)} = \mathbf{H}_k^{(i)} \mathbf{s}_k^{(i)} + \boldsymbol{\varepsilon}_k^{(i)}, \quad (13)$$

where $\mathbf{H}_k^{(i)}$ is the sub-matrix of $\mathbf{H}^{(i,0)}$ built from rows $\{k-D, \dots, k+D\}$ and columns $\{k-2D, \dots, k+2D\}$, and where $\boldsymbol{\varepsilon}_k^{(i)}$ denotes noise plus residual ICI and ISI. $\boldsymbol{\varepsilon}_k^{(i)}$ is modeled as zero-mean Gaussian with covariance $\boldsymbol{\Sigma}_{\boldsymbol{\varepsilon}_k}$. The proposed equalizer uses the system model in (13).

IV.2) Iterative Maximum Likelihood Equalizer (IMLE): Our equalizer uses the observation $\mathbf{x}^{(i)}$ and knowledge of $\mathbf{H}^{(i,0)}$ to update the i^{th} multicarrier symbol’s bit reliability metrics $\{L^{(i)}(k, m), \forall m\}_{k=0}^{N-1}$, also referred to as L -values (LVs).

$$L^{(i)}(k, m) := \ln \frac{P(c_{k,m}^{(i)} = 0 | \mathbf{x}^{(i)})}{P(c_{k,m}^{(i)} = 1 | \mathbf{x}^{(i)})} \quad (14)$$

Since all quantities pertain to the i^{th} multicarrier symbol, we can omit superscript indices w.l.o.g. Note that the sign of $L(k, m)$ is the uncoded MAP bit decision and the magnitude of $L(k, m)$ indicates the reliability of this decision. Using Bayes’ rule and assuming independent bits,³ $L(k, m)$ can be rewritten

³As a consequence of, e.g., interleaving.

as the sum of the prior LV, $L_o(k, m)$, and the extrinsic LV, $\Delta L(k, m)$, defined in (15).

$$L(k, m) = \ln \frac{\sum_{\gamma \in \mathcal{G}_{kN+m,0}^{NM}} p(\mathbf{x}|\mathbf{c} = \gamma) \prod_{\substack{k' \neq k \\ m' \neq m}} P(c_{k',m'} = \gamma_{k'N+m'})}{\sum_{\gamma \in \mathcal{G}_{kN+m,1}^{NM}} p(\mathbf{x}|\mathbf{c} = \gamma) \prod_{\substack{k' \neq k \\ m' \neq m}} P(c_{k',m'} = \gamma_{k'N+m'})} \underbrace{\Delta L(k, m)}_{\Delta L(k, m)} + \ln \frac{P(c_{k,m} = 0)}{P(c_{k,m} = 1)} \underbrace{L_o(k, m)}_{L_o(k, m)}.$$

Here, $\mathcal{G}_{k_2, \alpha}^{k_1}$ denotes the set of all length- k_1 bit vectors in which the k_2^{th} bit has been set to $\alpha \in \{0, 1\}$. The decoupling of $\Delta L(k, m)$ and $L_o(k, m)$ is important; we will ensure that $L_o(k, m)$ is not used in the calculation of $\Delta L(k, m)$.

Since exact computation of $\Delta L(k, m)$ is generally infeasible, we use a sub-optimal algorithm based on an approximation of $\Delta L(k, m)$ using only the partial observation \mathbf{x}_k (from (13)). This approximation will involve the symbol means $\{\mu_k\}$ and variances $\{v_k\}$ defined in (16)-(17).

$$\mu_k = \sum_{\beta \in \mathcal{S}} \beta P(s_k = \beta) \quad (16)$$

$$v_k = \sum_{\beta \in \mathcal{S}} |\beta|^2 P(s_k = \beta) - |\mu_k|^2 \quad (17)$$

The equalizer derives its name from the fact that $\Delta L(k, m)$ is the maximum likelihood (ML) decision statistic for bit $c_{k,m}$. Here, however, $\Delta L(k, m)$ is approximated to reduce computational complexity. The key idea is to first perform a soft interference cancellation (SIC) using the symbol means $\{\mu_k\}$, then to apply a Gaussian model to the residual interference-plus-noise. The resulting $\Delta L(k, m)$ approximation, denoted by $\tilde{\Delta L}(k, m)$, is much easier to compute. Specifically, the partial observation after SIC is written

$$\begin{aligned} \mathbf{y}_k &= \mathbf{x}_k - \mathbf{H}_k \boldsymbol{\mu}_k \\ &= \mathbf{h}_{k,0} s_k + \underbrace{\sum_{\substack{j=k-2D \\ j \neq k}}^{k+2D} \mathbf{h}_{k,j} (s_j - \mu_j)}_{\mathbf{q}_k} + \boldsymbol{\varepsilon}_k \end{aligned} \quad (18)$$

where $\mathbf{h}_{k,j}$ denotes the $(j+2D)^{\text{th}}$ column of \mathbf{H}_k and where

$$\boldsymbol{\mu}_k := [\mu_{k-2D}, \dots, \mu_{k-1}, 0, \mu_{k+1}, \dots, \mu_{k+2D}]^t. \quad (19)$$

The residual interference vector \mathbf{q}_k is modeled as zero-mean Gaussian, independent of s_k , with covariance $\boldsymbol{\Sigma}_{\mathbf{q}_k}$:

$$\boldsymbol{\Sigma}_{\mathbf{q}_k} = \sum_{\substack{j=k-2D \\ j \neq k}}^{k+2D} v_j \mathbf{h}_{k,j} \mathbf{h}_{k,j}^H + \boldsymbol{\Sigma}_{\boldsymbol{\varepsilon}_k}. \quad (20)$$

$$= \mathbf{H}_k \mathcal{D}(\mathbf{v}_k) \mathbf{H}_k^H + \boldsymbol{\Sigma}_{\boldsymbol{\varepsilon}_k} \quad (21)$$

where

$$\mathbf{v}_k := [v_{k-2D}, \dots, v_{k-1}, 0, v_{k+1}, \dots, v_{k+2D}]^t. \quad (22)$$

Replacing $p(\mathbf{x}|\mathbf{c} = \gamma)$ in (15) with $p(\mathbf{y}_k|s_k = \psi(\gamma))$, the extrinsic LV becomes

$$\tilde{\Delta L}(k, m) = \ln \frac{\sum_{\gamma \in \mathcal{G}_{m,0}^M} e^{\text{Re}(\psi(\gamma)g_k)} \prod_{m' \neq m} e^{\frac{(-1)^{\gamma_{m'}} L_o(k, m')}{2}}}{\sum_{\gamma \in \mathcal{G}_{m,1}^M} e^{\text{Re}(\psi(\gamma)g_k)} \prod_{m' \neq m} e^{\frac{(-1)^{\gamma_{m'}} L_o(k, m')}{2}}}$$

where $g_k := \mathbf{y}_k^H \boldsymbol{\Sigma}_{\mathbf{q}_k}^{-1} \mathbf{h}_{k,0}$.

The IMLE algorithm proceeds as follows. Prior to the first iteration, $\{L_o(k, m) \forall k, m\}$ are obtained from the output of a soft decoder, if available, or otherwise set to zero. These LVs are then used to initialize $\{\mu_k\}_{k=0}^{N-1}$ and $\{v_k\}_{k=0}^{N-1}$. We begin by working on symbol index $k = 0$. The means $\boldsymbol{\mu}_0$ and variances \mathbf{v}_0 are used to calculate \mathbf{y}_0 and $\boldsymbol{\Sigma}_{\mathbf{q}_0}$, which in turn are used to compute g_0 . From g_0 and $\{L_o(0, m)\}_{m=0}^{M-1}$, $\{\tilde{\Delta L}(0, m)\}_{m=0}^{M-1}$ are calculated and used to compute $\{L(0, m)\}_{m=0}^{M-1}$. Finally, $\{L(0, m)\}_{m=0}^{M-1}$ are used to update μ_0 and v_0 . The $k = 1$ case is tackled next, then $k = 2$, and so on, until $k = N - 1$. Finally, $\{L(k, m) \forall k, m\}$ are copied to $\{L_o(k, m) \forall k, m\}$. This concludes the first iteration. The algorithm terminates after a specified number of iterations.

The computational complexity for IMLE is dominated by the inversion of the $(2D+1) \times (2D+1)$ matrix $\boldsymbol{\Sigma}_{\mathbf{q}_k}$, yielding a per-iteration complexity order of $\mathcal{O}(ND^3)$. It is interesting to note that IMLE-BPSK is similar to the probabilistic data association (PDA)-based multi-user detection (MUD) schemes proposed in [9]. However, in [9], the iterative symbol detection strategy is applied *after* a zero-forcing (ZF) transformation is applied to \mathbf{x} , i.e., after the channel has been trivialized. Since the ZF transformation has a complexity order of $\mathcal{O}(N^3)$, it is much more costly than IMLE and IMSE since, typically, $D \ll N$. Essentially, IMLE leverages the banded structure of \mathbf{H} , while PDA does not. IMLE is also similar to [10]. However, our algorithm updates LVs for individual bits and passes bit LVs to the decoder, whereas soft symbol estimates are updated in [10] and bits are detected via hard decision on the final symbol estimate. Also note that whereas [10] works in the time-lag domain, our scheme operates in the frequency-doppler domain. This is advantageous since the number of interfering symbols is smaller for our scheme as $D \ll N_h$.

V. SIMULATION RESULTS

Here we characterize the performance of the proposed PS-FDM system employing IMLE and coding. End-to-end coded BER is used as a performance measure for the proposed iterative equalizer. The iterative equalizer is used in a turbo-equalizer configuration Fig. 3. As a reference, we use the *perfect global interference canceler* (PGIC) with one equalization and decoding iteration, in which the equalization step is IMLE for $\{L^{(i)}(k, m)\}_0^{M-1}$ assuming all interference $\{s_d^{(j)}\}_{(j,d) \neq (i,k)}$ is known perfectly. We also consider the *perfect local interference canceler* (PLIC). PLIC is similar to PGIC except that, when using IMLE for $\{L^{(i)}(k, m)\}_0^{M-1}$, only neighboring co-cursor ICI $\{s_d^{(i)}\}_{d=k-2D}^{k+2D}$ is known; ISI and non-neighboring ICI are unknown. This PLIC lower bounds the BER of the IMLE, since, in the best case, it too

cancel only local interference. The proximity of PLIC and PGIC performance curves measures the success of the pulse design's out-of-target interference suppression ability.

V.1) Setup: Experiments employed (Gray-mapped) QPSK constellations, SNR^{-1} -variance CWGN noise, a WSSUS Rayleigh-fading channel with uniform power profile (i.e., $\sigma_l^2 = N_h^{-1}$ for $0 \leq l < N_h$), and design choices $N_a = 1.5N_s$, $N_b = N_a + N_h/2$, and $D = \lceil f_d N \rceil + 1$. We chose $N = 64$, $N_h = 32$, and $N_s = N$ (i.e., no guard interval) and studied $f_d = 0.03$ and $f_d = 0.01$. Recall that f_d is normalized to the chip rate, i.e., $r_t(q) = J_0(2\pi f_d q)$. Channel knowledge was assumed and, hence, no pilots were employed. For purposes of coding, a (7, 5) rate- $\frac{1}{2}$ (non-systematic) convolutional code, along with a SISO BCJR decoder [13], was used.

V.2) Results and Discussion: Figure 4 depicts the performance of the system with max-SINR transmitter pulses and a standard CP-OFDM receiver window.

The BER is plotted against the ratio of information-bit energy to noise spectral density. In these BER plots, $\text{ML}k$ refers to IMLE with k decoding iterations. LIN refers to the performance of the MCM system with standard linear MMSE based equalization and one decoding iteration. WN refers to the performance of the convolutional code over a CWGN channel, representing performance in the absence of interference and fading.

In Fig. 4, the gap between the PLIC and PGIC curves is less than 1dB for all cases, implying that, with our pulse shapes and simplified system model (13), the loss in performance is small, even at the high Doppler frequency of $f_d = 0.03$. Also notice that, PGIC/PLIC for $f_d = 0.03$ is lower than $f_d = 0.01$. Recall that D increases with f_d and provides diversity gain at the cost of complexity.

We note that, as f_d increases, PGIC/PLIC performance improves (as a consequence of diversity) while IMLE performance degrades. We attribute this degradation to error propagation during iterative equalization. Even so, we find that IMLE performance is within 1.5dB the PLIC bound at $f_d = 0.03$. In both cases, it is clear that the algorithms perform significantly better than an $\mathcal{O}(N^3)$ standard non-iterative linear MMSE based equalization strategy. This is remarkable considering that the IMLE has $\mathcal{O}(ND^3)$ complexity.

VI. CONCLUSIONS

We presented a new approach to PS-FDM in the presence of doubly-dispersive fading. Pulse sequences were constructed to shape ICI/ISI into a pattern that enables low-complexity diversity-leveraging equalization, and a suitable equalization algorithm was described. Simulations demonstrated the efficacy of the proposed technique.

REFERENCES

- [1] S. B. Weinstein and P. M. Ebert, "Data transmission by frequency division multiplexing using the discrete Fourier transform," *IEEE Trans. Commun.*, vol. 19, pp. 628–634, Oct. 1971.
- [2] A. Stamoulis, S. N. Diggavi, and N. Al-Dhahir, "Intercarrier interference in MIMO OFDM," *IEEE Trans. Signal Processing*, vol. 50, pp. 2451–2464, Oct. 2002.

- [3] X. Cai and G. B. Giannakis, "Bounding performance and suppressing inter-carrier interference in wireless mobile OFDM," *IEEE Trans. Commun.*, vol. 51, pp. 2047–2056, Dec. 2003.
- [4] W. Burchill and C. Leung, "Matched filter bound for OFDM on Rayleigh fading channels," *Electronics Letters*, vol. 31, pp. 1716–1717, Sep. 1995.
- [5] A. M. Sayeed and B. Aazhang, "Joint multipath-doppler diversity in mobile wireless communications," *IEEE Trans. Commun.*, vol. 47, pp. 123–132, Jan. 1999.
- [6] P. Schniter, "On the design of non-(bi)orthogonal pulse-shaped FDM for doubly-dispersive channels," in *Proc. IEEE Int. Conf. Acoustics, Speech, and Signal Processing*, 2004.
- [7] P. Schniter, "Low-complexity equalization of OFDM in doubly-selective channels," *IEEE Trans. Signal Processing*, vol. 52, pp. 1002–1011, Apr. 2004.
- [8] M. Tüchler, A. Singer, and R. Koetter, "Minimum mean square error equalization using *a priori* information," *IEEE Trans. Signal Processing*, vol. 50, pp. 673–683, Mar. 2002.
- [9] D. Pham, J. Luo, K. R. Pattipati, and P. K. Willett, "A PDA-Kalman approach to multiuser detection in asynchronous CDMA," *IEEE Commun. Letters*, vol. 6, pp. 475–477, Nov. 2002.
- [10] S. Liu and Z. Tian, "Near-optimal soft decision equalization for frequency selective MIMO channels," *IEEE Trans. Signal Processing*, vol. 52, pp. 721–733, March 2004.
- [11] J. G. Proakis, *Digital Communications*. New York: McGraw-Hill, 4th ed., 2001.
- [12] P. Schniter, "A new approach to multicarrier pulse design for doubly-dispersive channels," in *Proc. Allerton Conf. Commun., Control, and Computing*, Oct. 2003.
- [13] L. R. Bahl, J. Cocke, F. Jelinek, and J. Raviv, "Optimal decoding of linear codes for minimizing symbol error rate," *IEEE Trans. Inform. Theory*, vol. 20, pp. 284–287, Mar. 1974.

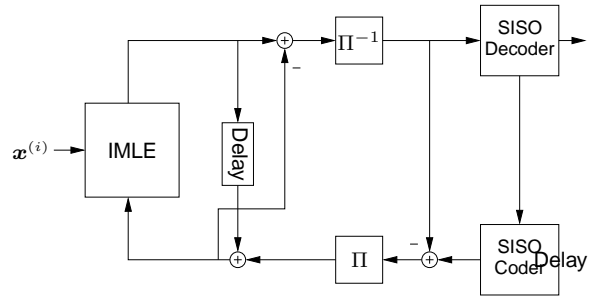


Fig. 3. Turbo receiver configuration.

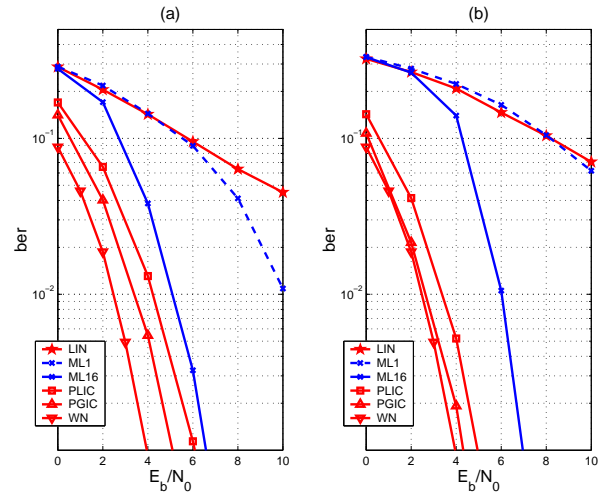


Fig. 4. QPSK with transmitter pulses and CP-OFDM receiver window for (a) $f_d = 0.01$ and (b) $f_d = 0.03$